Full-length Article

Interleukin-1β impedes oligodendrocyte progenitor cell recruitment and white matter repair following chronic cerebral hypoperfusion

Yiting Zhou [a,1], Jing Zhang [a,b,1], Lu Wang [a,1], Ying Chen [b], Yushan Wan [a], Yang He [a], Lei Jiang [a], Jing Ma [a], Rujia Liao [a], Xiangnan Zhang [a,c], Liyun Shi [d], Zhenghong Qin [e], Yudong Zhou [a], Zhong Chen [a,c,*], Weiwei Hu [a,c,*]

[a] Department of Pharmacology, Key Laboratory of Medical Neurobiology of the Ministry of Health of China, College of Pharmaceutical Sciences, School of Medicine, Zhejiang University, Hangzhou, Zhejiang 310058, PR China
[b] Department of Pharmacy, Sir Run Run Shaw Hospital, 3 East Qingchun Road, Hangzhou, Zhejiang 310016, PR China
[c] Collaborative Innovation Center for Diagnosis and Treatment of Infectious Diseases, Hangzhou, Zhejiang 310003, PR China
[d] Department of Basic Medical Science, Key Laboratory of Immunology and Molecular Medicine, School of Medicine, Hangzhou Normal University, Hangzhou, Zhejiang 310036, PR China
[e] Department of Pharmacology and Laboratory of Aging and Nervous Diseases, Soochow University School of Pharmaceutical Science, Suzhou 215123, PR China

ARTICLE INFO

ABSTRACT

Subcortical ischemic vascular dementia (SIVD) caused by chronic cerebral hypoperfusion exhibits progressive white matter and cognitive impairments. However, its pathogenetic mechanisms are poorly understood. We investigated the role of interleukin-1β (IL-1β) and its receptor IL-1 receptor type 1 (IL-1R1) in an experimental SIVD model generated via right unilateral common carotid arteries occlusion (rUCCAO) in mice. We found that IL-1β expression was elevated in the corpus callosum at the early stages after rUCCAO. IL-1 receptor antagonist (IL-1Ra), when delivered at an early stage, as well as IL-1R1 knockout, rescued the downregulation of myelin basic protein (MBP) and improved remyelination at the later stage after rUCCAO. Our data suggest that the recruitment of OPCs, but not the proliferation or differentiation of OPCs, is the only compromised step of remyelination following chronic cerebral ischemia. IL-1Ra treatment and IL-1R1 knockout had no effect on the oligodendrocyte progenitor cell (OPC) proliferation, but did promote the recruitment of newly generated OPCs to the corpus callosum, which can be reversed by compensatory expression of IL-1R1 in the SVZ of IL-1R1 knockout mice. Further, we found that recruited OPCs contribute to oligodendrocyte regeneration and functional recovery. In transwell assays, IL-1β inhibited OPC migration through IL-1R1. Moreover, KdPT which can enter the brain to block IL-1R1 also showed comparable protection when intraperitoneally delivered. Our results suggest that IL-1β during the early stages following chronic cerebral hypoperfusion impedes OPC recruitment via IL-1R1, which inhibits white matter repair and functional recovery. IL-1R1 inhibitors may have potential uses in the treatment of SIVD.

© 2016 Elsevier Inc. All rights reserved.

1. Introduction

As the second most prevalent type of dementia, vascular dementia is an important cause of intellectual decline in elderly people. Subcortical ischemic vascular dementia (SIVD), induced by chronic cerebral hypoperfusion as a result of small-artery disease, is a common subtype of vascular dementia (Kalaria et al., 2008). SIVD is often observed in patients with hypertension or atherosclerosis. Characteristic damage of SIVD includes progressive demyelination in white matter and deficiencies in cognitive abilities (Selnes and Vinters, 2006). Currently, there are no effective treatments for SIVD, a situation that is likely related to the dearth of information known about its pathogenetic mechanisms.

Demyelination takes place after chronic cerebral hypoperfusion and leads to axonal degeneration and progressive deterioration in neurological function (Gootjes et al., 2004; Selnes and Vinters, 2006; Wakita et al., 2002). However, if remyelination happens, the demyelinated axons can undergo ensheathment with new myelin sheaths, which can boost functional recovery (Liebetanz and Merkler, 2006). It is well established that amplification of the oligodendrocyte progenitor cell (OPC) pool in the white matter

can benefit remyelination and functional recovery, no matter whether this amplification occurs by increasing OPC proliferation or through recruiting cells to the lesion area (Arnett et al., 2001; Franklin and Goldman, 2015; Keirstead and Blakemore, 1999). Therefore, clarification of the pathological mechanisms related to remyelination may facilitate the discovery of new therapeutic targets for SIVD.

Previous research has implied that both activated microglia and reactive astrocytes participate in the development of the white matter damage that is caused by chronic cerebral hypoperfusion (Yoshizaki et al., 2008). Inhibition of the activation of microglia and astrocytes is associated with the alleviation of white matter rarefaction and cognitive ability deficiency following chronic cerebral hypoperfusion (Ma et al., 2012). Interleukin-1β (IL-1β) is a major proinflammatory cytokine secreted by glia; it has been suggested that IL-1β is involved in acute focal cerebral ischemia (Huang et al., 2006). In vascular dementia patients, the level of IL-1β in plasma was higher than in controls (Zuliani et al., 2007). It is known that oligodendrocyte and OPC express IL-1 receptor type 1 (IL-1R1), a receptor for IL-1β (Vela et al., 2002). A previous study demonstrated that IL-1β promotes oligodendrocyte differentiation through the induction of insulin-like growth factor 1 under cuprizone-induced demyelination (Mason et al., 2001). In contrast, others reported that IL-1β alters the developmental program of white matter by inhibiting the oligodendrocyte maturation process in postnatal mice (Favrais et al., 2011). Although IL-1β appears to show inconsistent effects on oligodendrocyte generation in different biological contexts, these studies seem to suggest that IL-1β participates in remyelination following chronic cerebral hypoperfusion-induced white matter damage.

In the present study, we set out to explore the role of IL-1β and its receptor IL-1R1 in SIVD. We were particularly interested in its possible role in the remyelination process. We conducted experiments using a mouse model of chronic cerebral hypoperfusion; this model is established via right unilateral common carotid arteries occlusion (rUCCAO). It leads to the activation of glial cells, loss of oligodendrocyte and progressive demyelination, and replicates the white matter injuries and cognitive behavior deficient in SIVD (Ma et al., 2012, 2015; Yoshizaki et al., 2008).

2. Materials and methods

2.1. Animal preparation and surgery

All experiments were approved by and conducted in accordance with the ethical guidelines of the Zhejiang University Animal Experimentation Committee and were in complete compliance with the National Institutes of Health Guide for the Care and Use of Laboratory Animals. Efforts were made to minimize any pain or discomfort, and the minimum number of animals was used. Male 8–9 weeks old wild-type (WT, C57BL/6 strain) and IL-1R1$^{-/-}$ mice (C57BL/6 background) were administered with sodium pentobarbital (60 mg/kg) for anesthesia. The right common unilateral carotid artery was isolated from the adjacent vagus nerve and double-ligated with 6-0 silk sutures to cut off to achieve rUCCAO. Sham-operated mice were subjected to the same procedure, except for carotid ligation. Mice were subjected to novel object recognition test and Morris water maze test during D28 to D34 or sacrificed on D1, D3, D7, D8, D14 or D34 after rUCCAO for Western blot assay, on D8 or D34 for immunostaining examination and on D34 for compound action potentials (CAP) recording.

2.2. Drug administration

Mice were intracerebroventricular injected with saline, IL-1 receptor antagonist (IL-1Ra, Prospec, NJ, USA; 1 μg in 1 μl saline per day) or IL-1β (Prospec, NJ, USA; 3 ng in 1 μl saline per day) through a guide cannula (62003, RWD Life Science Co., Ltd) from D1 to D7 after rUCCAO. The guide cannula was stereotaxically implanted into the lateral ventricle (AP: −0.5 mm, L: −1.0 mm, V: −2 mm) a week before surgery. To study cell proliferation, mice were injected with BrdU (Sigma, USA; 100 mg/kg, i.p.) twice per day for 3 consecutive days after rUCCAO, and were sacrificed on D8. KdPT or saline was intraperitoneally injected (Bachem, Switzerland; 1 or 5 mg/kg, i.p.) from D1 to D7 after rUCCAO.

2.3. Novel object recognition test

As previously described (Ma et al., 2012, 2015), a glass box (30 × 45 × 30 cm) and three objects that were in three different shapes and colors were used in the test. On the first day of the test, the mice were allowed to explore the box without any objects for 10 min. Next day, there were two trials, and the intertribal interval was 1 h. In the first trial, two identical objects were presented on two opposite sides of the box, and the mouse was placed in the box and allowed to explore for 10 min. During the second trial, one of the objects presented in the first trial was replaced with a new object and the mice were allowed to explore for 3 min. Exploration was considered as directing the nose at a distance <1 cm from the object and/or touching it with the nose. The exploration time spent on each of the familiar (F) object and the new (N) object was recorded manually in blind manner. Discrimination index was calculated by (N − F/N + F) × 100% for intergroup comparison.

2.4. Morris water maze test

As reported before (Ma et al., 2012, 2015), a circular pool, with a diameter 150 cm and a height 50 cm, was filled with water at a depth of 30 cm. A hidden platform was submerged 1.5 cm below the surface of the water. At the acquisition phase, each mouse was trained 4 trials per day for 4 days, and the interval between the trials was 10 min. During each trial, the escape latency as the time to reach the platform and climb up out of the water was recorded, but limited to 60 s. On the fifth day, each mouse was tested in a probe trial, by removing the platform from the pool, and the time they stayed in the quadrant of the platform was recorded.

2.5. Western blot assay

The corpus callosum of mice after rUCCAO was carefully separated. Western blot was carried out by standard protocol with proper antibodies (Ma et al., 2015). Primary antibodies include: rabbit anti-IL-1β (1:1000; Abcam, UK), rat anti-myelin basic protein (anti-MBP; 1:500; Millipore, USA), and anti-GAPDH (1:5000; Kang-chen, China).

2.6. Immunofluorescent staining

Mice were perfused transcardially with 4% paraformaldehyde (PFA) in 0.1 M phosphate buffer (PBS, pH 7.4). Frozen brain sections (20 μm) were obtained by a cryostat (SM2000R, LEICA, Wetzlar, Germany). Sections then blocked with donkey serum for 2 h and incubated with primary antibodies overnight at 4 °C. Next day, sections were incubated with secondary antibodies for 2 h at room temperature. Primary antibodies included the followings: rabbit anti-IL-1β (1:200; Abcam, UK), rat anti-MBP (1:250; Millipore, USA), rabbit anti-Olig2 (1:500; Millipore, USA), mouse anti-Olig2 (1:300; Millipore, USA), rabbit anti-NG2 (anti-NG2 chondroitin sulfate proteoglycan; 1:300; Abcam, UK), mouse anti-proliferating cell nuclear antigen (anti-PCNA; Genentech, USA), rabbit anti-Ki67 (1:200; Abcam; UK) and mouse anti-BrdU (1:1000; Sigma, USA).

Secondary antibodies included the followings: AlexaFluor-488-, AlexaFluor-594-secondary antibodies to rabbit, rat or mouse (1:400). Nuclei were counterstained with DAPI. Fluorescent images were collected on a fluorescence microscope (BX51, Olympus, Japan) or a laser confocal scanning microscope (FV1000, Olympus, Japan). The fluorescence intensity analysis and cell counting were performed by Image J software (NIH, MD, USA) in the ipsilateral corpus callosum from three slices at the similar coronal position of each animal. IL-1β+/GFAP+, IL-1β+/Iba-1+, NG2+/DAPI+ or NG2+/BrdU+ double positive cells were counted by a blind manner. In the ipsilateral subventricular zone (SVZ), the PCNA+/NG2+, Ki67+/Olig2+ or BrdU+/NG2+ double positive cells were counted from four slices at the similar coronal position (AP = 0.5 mm) of each mouse by a blind manner. The cell numbers were then corrected by the analyzed size.

2.7. Retrovirus and adenovirus Injection

Newly generated cells in SVZ were traced with a pROV-EF1a-GFP retrovirus (Neuron Biotech, China) by direct injection in SVZ (AP = 0.5 mm, RL = 1.5 mm, H = −2.5 mm). Retroviral stock of 1 µl was injected (titer 4×10^8 cfu/ml) in 8 min at 3 d before rUCCAO. Adenovirus *IL-1R1-RFP* or vector-*RFP* (0.3 µl, titer 1×10^8 cfu/ml, Vigene, USA) was delivered to SVZ in *IL-1R1$^{-/-}$* mice together with 1 µl retrovirus before rUCCAO. Mice were sacrificed at 8 d after surgery, and coronal tissue sections (30 µm thick) were obtained and stained with rabbit anti-Olig2 (1:500; Millipore, USA). Z-stacks of 2 µm-thick single-plane images over the entire slice were captured using confocal microscope (Olympus, Japan). Four consecutive slices at the similar coronal position (AP = 0.5 mm) were taken for observation from each animal. The cell numbers in corpus callosum were counted and then corrected by the analyzed size.

2.8. Electron microscopy

Mice were transcardially perfused with a fixation buffer containing 2.5% glutaraldehyde and 4% paraformaldehyde. Samples of the middle segment of corpus callosum ipsilateral to the occluded carotid were obtained and kept in the same buffer for 48 h at 4 °C. After that, samples were postfixed in 1% osmium tetroxide, dehydrated in cold ethanol, infiltrated and embedded in Epon812. Sections of 120 nm were then collected, placed on grids, and stained with uranyl acetate and lead citrate. The grids were then imaged using a transmission electron microscope. Myelinated axons quantification was performed on 12 images per animal. G ratios (the ratio of axon diameter to the axon plus myelin sheath diameter) were calculated using Image J software for at least 150 fibers per animal.

2.9. Transwell chamber assays

Primary OPCs cultures were obtained from postnatal D2 Sprague-Dawley rats, as described previously (Hayakawa et al., 2011). We used a 8-µm pore-sized transwell based Boyden chamber system (Corning Incorporated, USA) to perform OPCs migration assays as described (Anliker et al., 2013). After both sides of the transwell membrane were pre-coated with poly-D-lysine, OPCs were seeded in up-side of the membrane at ~100,000 per well and maintained in 200 µl neurobasal medium with supplement of Ara-C (5 µM, Sangon Biotech, China) to prevent the proliferation. IL-1β (1, 10 or 100 ng/ml, Prospec, NJ, USA) was added to the lower or both upper and lower chamber. Platelet-derived growth factor (PDGF, 10 ng/ml, PeproTech, NJ, USA), IL-1Ra (10 ng/ml, Prospec, NJ, USA), NSC23766 (1 µM, Santa Cruz, USA) or Rho inhibitor I (0.25 µg/ml, Cytoskeleton, CO, USA) were added to the lower

chamber. OPCs were allowed to migrate for 24 h. After fixed with 4% PFA, non-migrated cells were wiped out of the top compartment with a cotton swab and migrated cells were stained with Crystal Violet Staining Solution (Beyotime, China). The migrated cells were counted in 8 randomly selected microscopic fields from each well (each treatment run in double wells for 3–4 individual experiments). The final results were presented as relative mean number to controls.

2.10. CAP recording

The brains were quickly removed and placed in ice-cold slicing solution containing the following: 87 mM NaCl, 2.5 mM KCl, 1.25 mM NaH$_2$PO4, 25 mM NaHCO$_3$, 25 mM glucose, 75 mM sucrose, 7 mM MgCl$_2$ and 0.5 mMCaCl$_2$, bubbled in 95% O$_2$, 5% CO$_2$ (pH 7.4). Coronal slices 350 mm thickness were obtained using a VT1000S Vibratome (Leica) and placed for 30 min in an incubating chamber containing ACSF (119 mM NaCl, 2.5 mM KCl, 1 mM NaH$_2$PO4, 26 mM NaHCO$_3$, 11 mM glucose, 1.3 mM MgCl$_2$ and 2.5 mM CaCl$_2$). Slices were then kept in the same recording solution at room temperature (22–25 °C) for 1–2 h until time for electrophysiological analysis. Slices were placed in a recording chamber superfused with oxygenated recording solution at a flow rate of 3 ml/min and viewed using the 10× objective of an Olympus BX61WI microscope. Extracellular field electrodes with a tip resistance of 2 MΩ were filled with ACSF and CAP were evoked using a glass electrode connected to a constant current isolated stimulator DS3 (Digitimer; 300–400µA). We systematically placed the stimulating electrode at the ipsilateral side of corpus callosum and recorded in the median. Two distinguishable waves were produced by axon conduction velocities. The first corresponds to myelinated (M) axons and the second corresponds to unmyelinated (UM) axons. The maximum CAP amplitude for both the M and UM waves were used for analysis, and the percentage of amplitude for M was calculated. To measure conduction velocity for the M wave, the time duration (in milliseconds) to reach maximum amplitude from baseline was determined.

2.11. Statistical analysis

All data were collected and analyzed in a blind fashion. Data are presented as means ± SEM. The multiple comparisons were analyzed by One-way ANOVA followed by *Tukey* test. A general linear model was used to analyze the difference in latency among different treatment groups in Morris water maze test, with the consideration of all the test days. For all analyses, the tests were two-sided and a $P < 0.05$ was considered significant.

3. Results

3.1. High expression of IL-1β at early stage following chronic cerebral hypoperfusion impedes remyelination for white matter repair

Western blot assays and ELISA demonstrated that IL-1β expression in the corpus callosum increased during D1-D7 after rUCCAO but returned to the baseline thereafter (Fig. 1A, B). Immunostaining confirmed the change of the IL-1β level in the corpus callosum (Fig. 1C) and showed that most IL-1β positive cells were co-localized with either the astrocyte marker GFAP or the microglia marker Iba1 (Fig. 1D, 40.03 ± 0.97% vs. 47.77 ± 4.44%, n = 4–5). These results suggest that glia-derived IL-1β expression was increased robustly at the early stages following rUCCAO. This increase occurred locally; there was no alteration of IL-1β expression in other brain regions such as the cortex or the hippocampus (Supplementary Fig. 1).
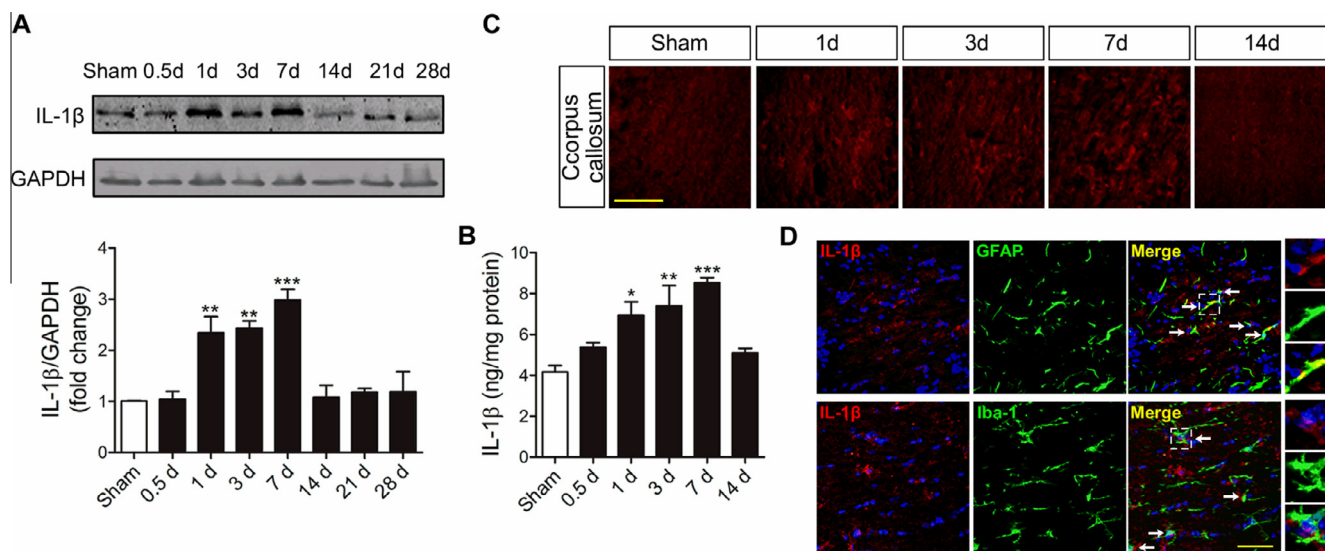
Fig. 1. IL-1β expression increases at the early stages after chronic cerebral hypoperfusion. The IL-1β expression in the corpus callosum was evaluated at different time points after rUCCAO by Western blot analysis (A, the mature form of IL-1β with a band at ~17 kDa), ELISA (B) and immunostaining (C, D: 3d after rUCCAO). The dotted line in C represents the boundaries of the corpus callosum. Double staining (arrows) of IL-1β (red) and GFAP (green) or Iba-1 (green) in the corpus callosum is shown in D. The cells in the boxed portion are enlarged in the insets. LV, lateral ventricle. Scale bar, 50 μm. n = 4–5 for each group. Data are represented as means ± SEM. **$P < 0.01$, ***$P < 0.001$, vs. the sham group. (For interpretation of the references to color in this figure legend, the reader is referred to the web version of this article.)

It is thought that IL-1β signaling is mediated exclusively by IL-1R1. To understand the possible role of IL-1β and IL-1R1 in the pathological progress of white matter damage following chronic cerebral hypoperfusion, IL-1Ra, a competent antagonist of IL-1R1, and $IL-1R1^{-/-}$ mice were used. Immunostaining results revealed that MBP expression declined dramatically 34 d after rUCCAO, and the intracerebroventricular administration of IL-1Ra at an early stage after rUCCAO reversed this down-regulation of MBP expression (Fig. 2A, $P < 0.05$). The mice that lacked IL-1R1 had no reduction of MBP expression as compared with controls on D34 (Fig. 2A), while an increase in IL-1β expression after rUCCAO was observed in the $IL-1R1^{-/-}$ mice (Supplementary Fig. 2). A quantitative analysis of MBP expression by Western blot showed consistent results with the immunostaining experiments (Fig. 2B). To further examine the role of IL-1β and IL-1R1 in white matter damage, the myelin ultrastructure of the corpus callosum was evaluated by electron microscopy. The percentage of myelinated axons in mice exposed to rUCCAO decreased compared to a sham group on D34 (Fig. 2C, D); IL-1Ra administered at an early stage after rUCCAO reversed this decrease. $IL-1R1^{-/-}$ mice suffering from chronic cerebral ischemia did not show this change in myelination status. We then characterized all of the myelinated axons into two groups: thin myelinated axons ($0.8 < $ G-ratio < 1, indicating remyelinated axons and thick myelinated axons (G-ratio $\leqslant 0.8$, indicating preserved myelinated axons); unmyelinated axons had a G-ratio of 1 (Fig. 2C, E). We found that the percentage of thick myelinated axons was reduced following rUCCAO ($P < 0.001$); the percentage of thin axons did not change. Although both IL-1Ra treatment and IL-1R1 knockout did not affect axons of the thick myelinated group ($P > 0.05$), these treatments both strikingly improved the percentage of thin myelinated axons (i.e., remyelinated axons) ($P < 0.05$ and $P < 0.01$, respectively). In addition, to exclude the possibility that the increase in the percentage of myelinated axons resulting from blocking IL-1R1 was due to the alleviation of demyeliation, the myelin ultrastructure was also examined at an early stage after rUCCAO, when complete remyelination cannot possibly have occurred (Supplementary Fig. 3). We found that demyelination already appeared by 8 d after rUCCAO, while neither IL-1Ra nor IL-1R1 knockout had any effect on the

demyelination of axons. Additionally, TUNEL analysis of oligodendrocyte apoptosis and western blot analysis of cleaved caspase-3 expression in corpus callosum revealed that the apoptosis status was unchanged after IL-1Ra treatment (Supplementary Fig. 4). Taken together, these results suggest that blocking IL-1R1 alleviates the white matter damage that occurs following chronic cerebral hypoperfusion, possibly through a promotion of remyelination, but not through the preservation of myelin. It also implies that high expression of IL-1β at early stage following chronic cerebral hypoperfusion impedes remyelination for white matter repair.

3.2. IL-1β via IL-1R1 reduces the OPC pool in the corpus callosum following chronic cerebral ischemia by inhibiting SVZ-derived OPC recruitment to the corpus callosum

A large pool of OPCs is present in the white matter and SVZ. These cells have the ability to successfully replace damaged oligodendrocytes through proliferation, migration, differentiation, and remyelination following injury (El Waly et al., 2014; Kako et al., 2012). We found a significant reduction in the density of OPCs (NG2+ cells) in the corpus callosum at 8 d after rUCCAO (Fig. 3A, B, $P < 0.001$). This reduction was reversed by a treatment of IL-1Ra. $IL-1R1^{-/-}$ mice that received rUCCAO did not exhibit this decline. These results indicate that blocking IL-1R1 expands the OPC pool in the corpus callosum after rUCCAO.

As proliferation is the first step in remyelination, both PCNA and Ki67 immunostaining were performed to label the OPCs undergoing proliferation. We found that proliferating OPCs were almost exclusively present in SVZ and were not present in the injured corpus callosum (Fig. 3C). Unexpectedly, the number of proliferating OPCs did not decline, but increased remarkably in SVZ at 8 d after rUCCAO (Fig. 3C–F); this did not change after IL-1Ra treatment. $IL-1R1^{-/-}$ mice also displayed a comparable increase to that of WT mice after rUCCAO. Double immunostaining of BrdU and NG2 labels all of the newly generated OPCs, even those that have exited the cell cycle. These experiments revealed that the number of newly generated OPCs in SVZ was elevated following chronic cerebral hypoperfusion (Fig. 3G, H). Additionally, no further increase of newly generated OPCs in SVZ was observed in IL-1Ra treated mice.
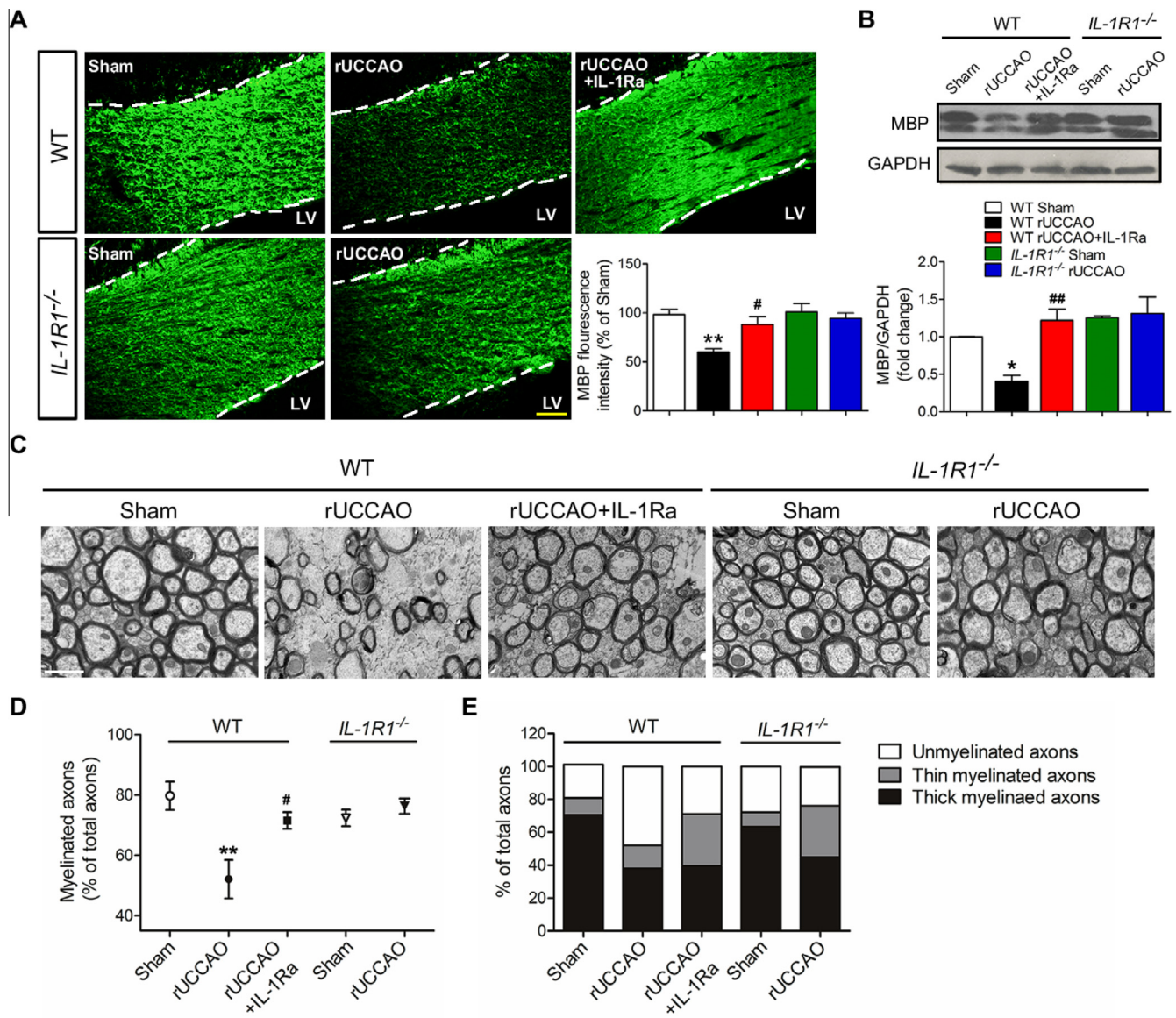
Fig. 2. Inhibition of IL-1R1 alleviates white matter damage and improves remyelination following chronic cerebral hypoperfusion. White matter and myelin damage was evaluated in terms of MBP expression (A: immunostaining; B: western blot) and electron microscopy (C–E) at 34 d after rUCCAO. The percentage of myelinated axons was calculated in D, and the distribution of axons according to their G-ratio values are shown in E (G-ratio $\leqslant$ 0.8, thick myelinated axons; 0.8 < G-ratio < 1, thin myelinated axons; G-ratio = 1, unmyelinated axons). The dotted line in A represents the boundary of the corpus callosum. LV, lateral ventricle. Scale bar: 50 μm in A and 1 μm in C. n = 5 in A, n = 4 in B and n = 3–4 in C–E. Data are represented as means ± SEM. $^*P < 0.05$, $^{**}P < 0.01$, vs. the sham group in WT mice; $^\#P < 0.05$, $^{\#\#}P < 0.01$, vs. the rUCCAO group in WT mice.

$IL\text{-}1R1^{-/-}$ mice had similar numbers of newly generated OPCs as the WT mice after rUCCAO. Thus, we hypothesized that the improvement in remyelination following IL-1R1 inhibition might be due to an increase in the OPC recruitment, rather than an increase in OPC proliferation.

In the corpus callosum, we did find that mice treated with IL-1Ra had expanded population of newly generated OPC (Brdu+/NG2+) as compared with the rUCCAO group mice at 8 d after surgery (Fig. 4A, B). $IL\text{-}1R1^{-/-}$ mice exhibited increased number of newly generated OPC in the corpus callosum compared with WT mice after rUCCAO. To eliminate the contribution of proliferating OPCs resident in the corpus callosum, we selectively labeled SVZ-derived newly generated cells via a replication-incompetent GFP retrovirus. GFP labeled cells were only detected in the region of SVZ; they were scarcely found in the corpus callosum of the sham group. In mice that received rUCCAO, a few GFP labeled cells were found in the corpus callosum at 8 d after rUCCAO. Of note, the number of GFP+ cells in the corpus callosum increased strikingly after treatment with IL-1Ra (Fig. 4C, D). This increase could be aborted when mice were co-injected with IL-1β in the lateral ventricle. In addition, after rUCCAO, $IL\text{-}1R1^{-/-}$ mice had more GFP + cells in the carpus callosum than did WT mice. To further confirm the contribution of IL-1R1 in the blockage of the recruitment of SVZ-derived cells, IL-1R1 expression was rescued in SVZ of $IL\text{-}1R1^{-/-}$ mice via adenovirus infection. The compensatory expression of IL-1R1 by the delivery of adenovirus *IL-1R1-RFP* in the SVZ of $IL\text{-}1R1^{-/-}$ mice reduced the population of retrovirally-labeled recruited (RFP+/GFP+) cells in the corpus callosum compared with controls (administered with adenovirus vector-*RFP*) at 8 d after rUCCAO (Fig. 4E, F). Since NG2 is also expressed in the pericytes in developing vasculature (Ozerdem et al., 2001), simultaneous immunostaining with Olig2, which labels both OPCs and their derived cells here, was performed to confirm the effects of IL-1β/IL-1R1 on SVZ-derived OPC recruitment (Fig. 4D–F). This result
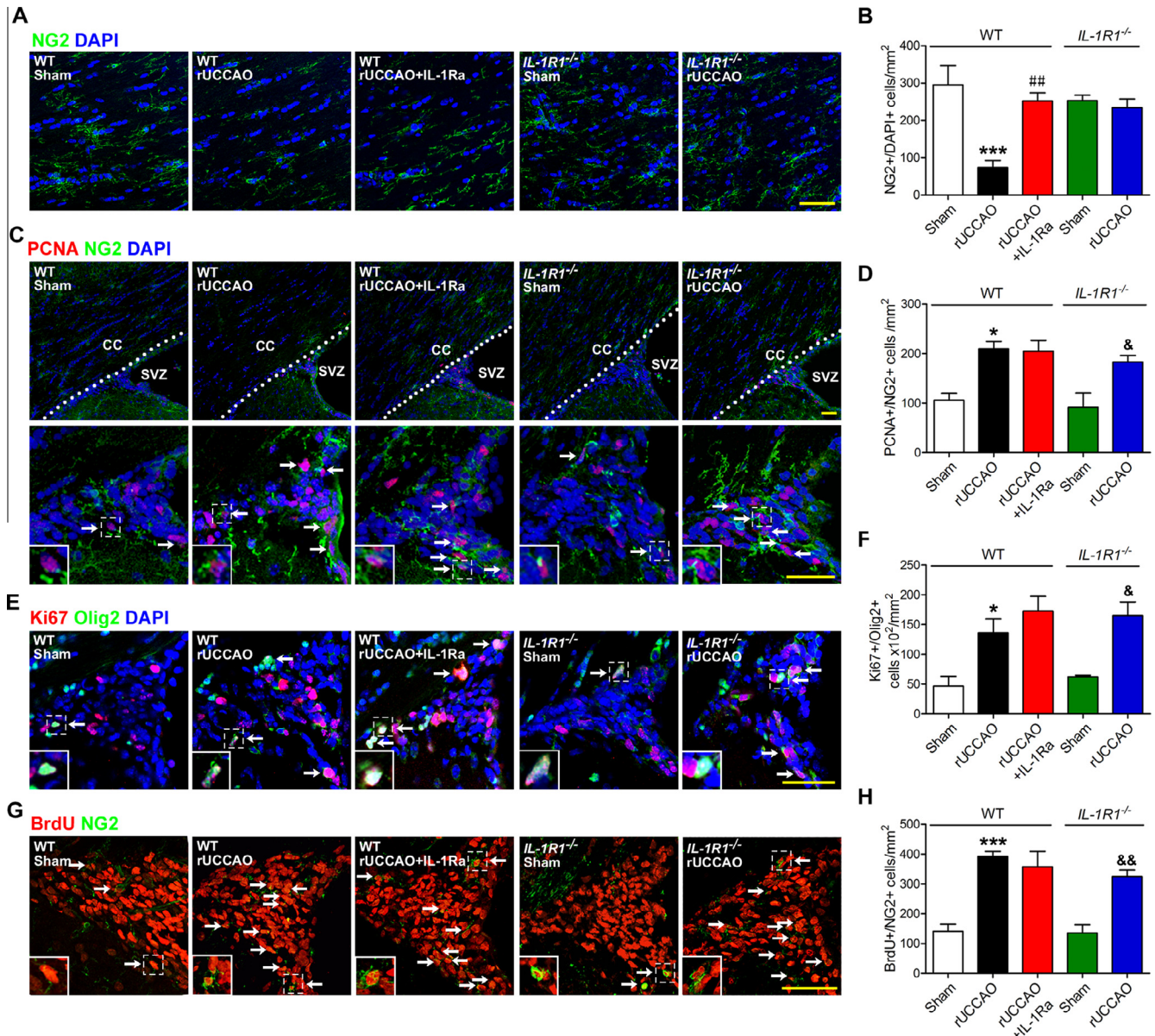
Fig. 3. Inhibition of IL-1R1 increases the number of OPCs in the corpus callosum but has no effect on the proliferation of OPCs in SVZ following chronic cerebral hypoperfusion. The number of OPCs (NG2+) in the corpus callosum at 8 d after rUCCAO was calculated in B, with representative photomicrographs in A. The effect of IL-1R1 blocking on OPC proliferation in SVZ at 8 d after rUCCAO was evaluated by PCNA/NG2 (C, D: the dotted line in the upper panel represents the boundary between SVZ and the corpus callosum; photomicrographs in the lower panel were enlarged from SVZ in the upper panel) and Ki67/Olig2 double immunostaining (E, F), with representative photomicrographs in C and E. The effect of IL-1R1 blocking on OPC proliferation in SVZ at 8 d after rUCCAO was evaluated by BrdU and NG2 double staining (G, H). BrdU (100 mg/kg, i.p., twice per day) was administrated as 3 consecutive days after rUCCAO. The double PCNA+/NG2+, Ki67+/Olig2+ or NG2+/BrdU+ cells are shown with arrows in C, E, G (the cells in the boxed portion are enlarged in the insets). Scale bar, 50 μm; n = 4–5. Data are represented as means ± SEM. $^*P < 0.05$, $^{**}P < 0.01$, $^{***}P < 0.001$, vs. the sham group in WT mice; $^{##}P < 0.01$ vs. the rUCCAO group in WT mice; $^{&}P < 0.05$, $^{&&}P < 0.01$, vs. the sham group in $IL\text{-}1R1^{-/-}$ mice.

suggests that IL-1β via IL-1R1 reduces the OPC pool in the corpus callosum following chronic cerebral ischemia by inhibiting SVZ-derived OPC recruitment to the corpus callosum, but does not affect OPC proliferation.

To directly confirm the effect of IL-1β/IL-1R1 on OPC migration, we adopted a popular *in vitro* model, transwell chamber assay. In this experiment, we added PDGF (10 ng/ml) into the lower chamber to entice OPCs to cross the filter in order to mimic spontaneous

Fig. 4. Inhibition of IL-1R1 promotes SVZ-derived OPC recruitment to the corpus callosum following chronic cerebral hypoperfusion. The number of newly generated OPCs (double NG2+/BrdU+) in corpus callosum at 8 d after rUCCAO was calculated in B, with representative photomicrographs in A. The arrows in A indicate newly generated OPCs (the cells in the boxed portion are enlarged in the insets). The retrovirally-labeled GFP+ recruited cells and the double Olig2+/GFP+ recruited OPCs in the corpus callosum were counted at 8 d after rUCCAO (D), with representative photomicrographs in C. The dotted lines in C represent the boundary of the corpus callosum (CC) and the cells in the boxed portion are enlarged in the insets. After the compensatory expression of IL-1R1 in $IL\text{-}1R1^{-/-}$ mice by injection of adenovirus (Adv) $IL\text{-}1R1\text{-}RFP$ into the SVZ (AP = 0.5 mm, RL = 1.5 mm, H = −2.5 mm), the retrovirally-labeled recruited (double RFP+/GFP+) cells and the recruited OPCs (triple RFP+/GFP+/Olig2+) were counted at 8 d after rUCCAO (F), with representative photomicrographs in E (the cells in the boxed portion are enlarged in the right panel). Scale bar, 50 μm. n = 5. Data are represented as means ± SEM. $^{***}P < 0.001$ vs. the rUCCAO group in WT mice; $^{###}P < 0.001$ vs. the IL-1Ra group in WT mice; $^{&&&}P < 0.001$ vs. the sham group in $IL\text{-}1R1^{-/-}$ mice; ΔP < 0.05, ΔΔP < 0.01 vs. the Adv vector-RFP rUCCAO group in $IL\text{-}1R1^{-/-}$ mice.

migratory behavior that occurs following white matter damage (Fig. 5A). IL-1β reduced the number of migrated OPCs in a dose dependent manner (Fig. 5C). To exclude the possibility that this reduction in migration resulted from a change in OPC motility, IL-1β was added into both the upper and lower chambers (Fig. 5A, D). In this case, there was no reduction in OPC migration, a result that clearly suggests IL-1β inhibits OPC chemotactic migration but not OPC motility (Fig. 5D). Rho GTPases, including RhoA, Rac1, and CDC42, are known to play central roles in cell migration (Le Clainche and Carlier, 2008). RhoA and Rac1 are likely to be
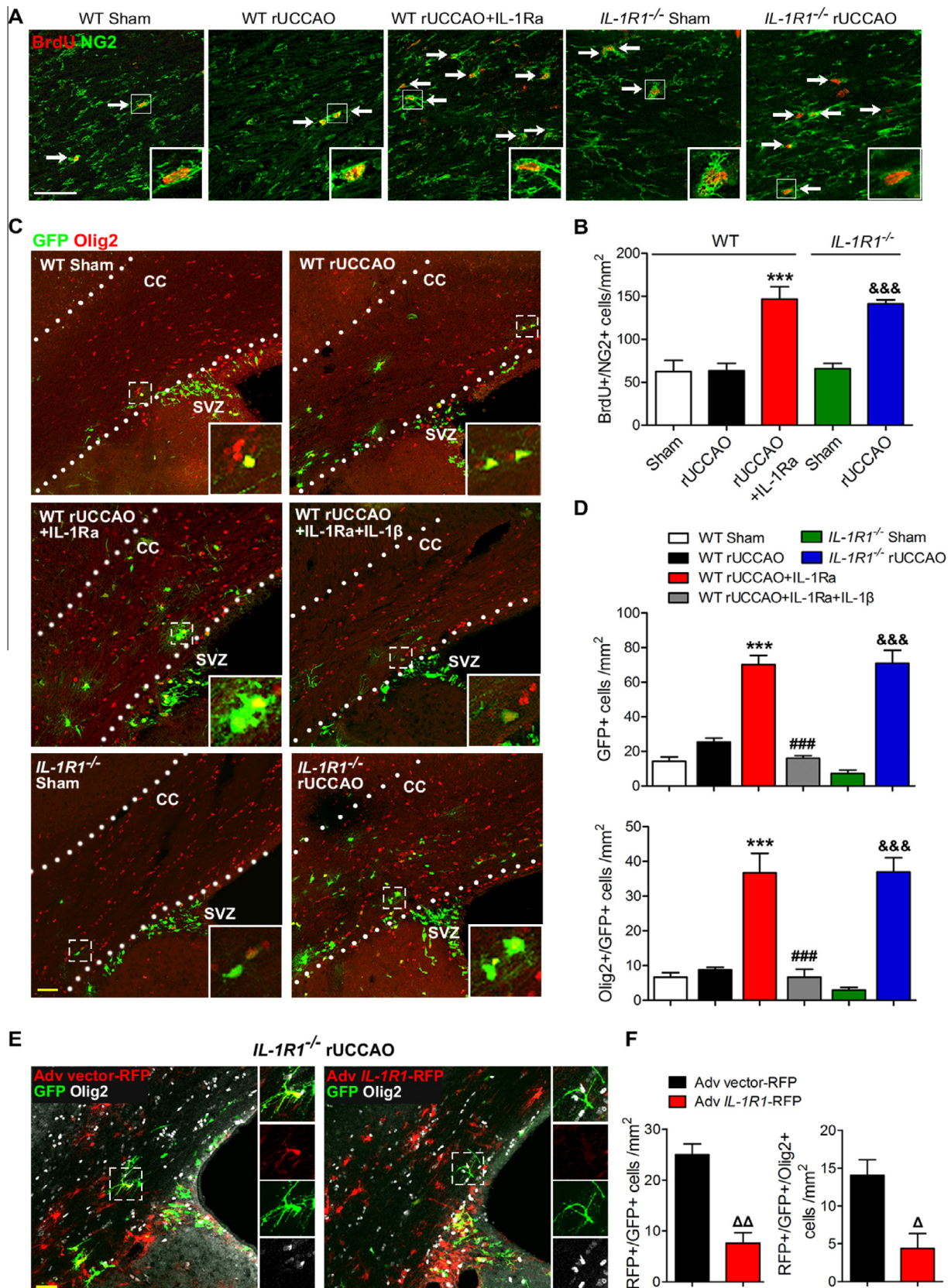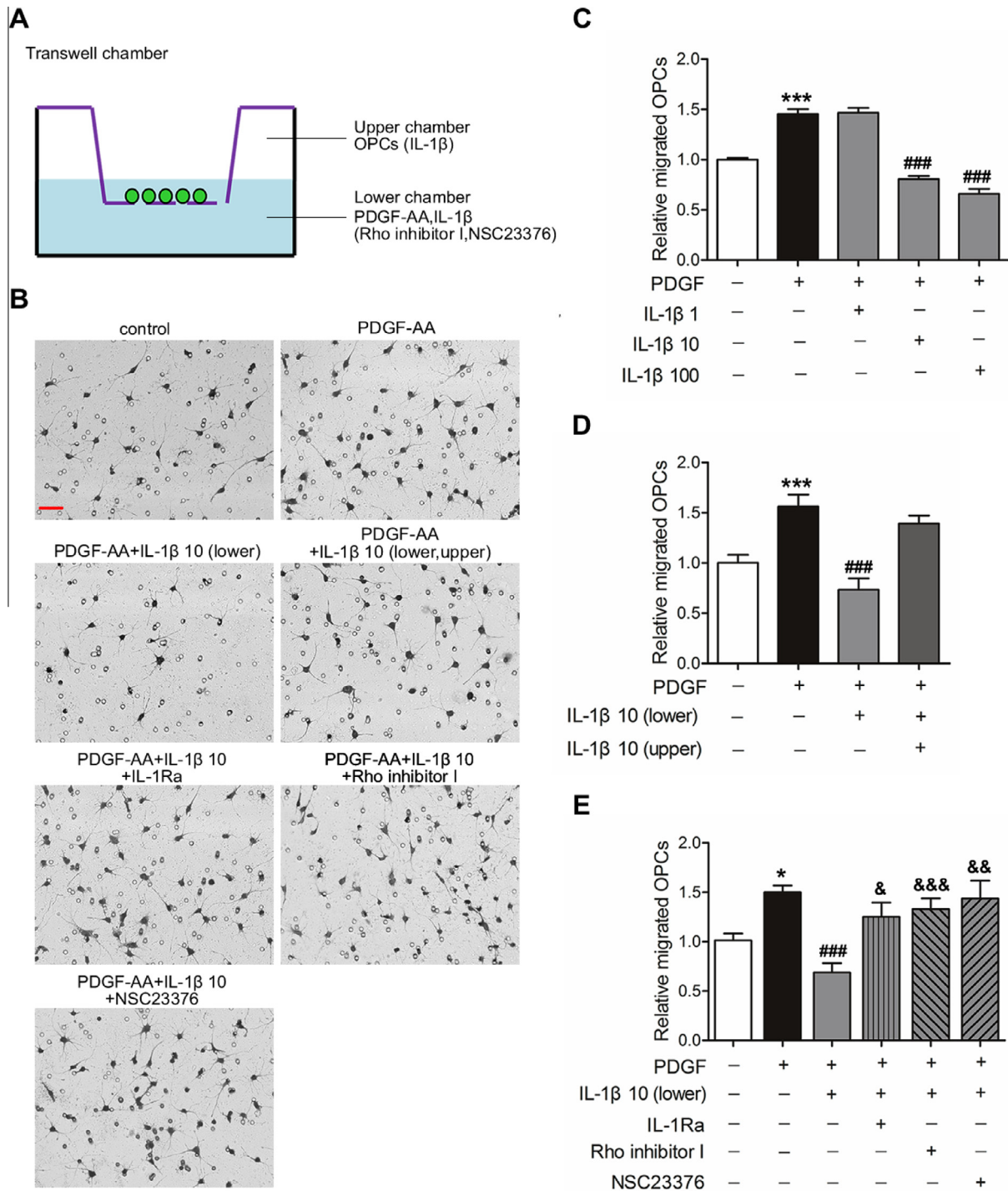
Fig. 5. IL-1β suppresses OPC migration in transwell chamber assays. The cartoon in A shows the drug administration protocol. PDGF (10 ng/ml) was added to the lower chamber to induce the migration of OPC. OPC migration was then assayed under varying doses of IL-1β (1, 10, or 100 ng/ml) added in the lower chamber (C). OPC motility was assayed when 10 ng of IL-1β was added to both the upper and lower chambers (D). OPC migration was assayed when IL-1Ra (10 ng/ml), NSC23766 (1 μM), or Rho inhibitor I (0.25 μg/ml) was added, together with IL-1β (10 ng/ml) in the lower chamber (E). Representative photomicrographs of migrated OPCs are shown in B. Values are from 3 to 4 independent experiments and are represented as means ± SEM. $^*P < 0.05$, $^{***}P < 0.001$ vs. controls; $^{##}P < 0.01$, $^{###}P < 0.001$ vs. PDGF group; $^{\&}P < 0.05$, $^{\&\&}P < 0.01$, $^{\&\&\&}P < 0.001$ vs. IL-1β group. Scale bar, 50 μm.

effectors in IL-1R1 signaling (Singh et al., 1999). We found that the inhibition of OPC migration provided by IL-1β could be abrogated by IL-1Ra, Rho inhibitor I (RhoA inhibitor), or NSC23766 (Rac1 inhibitor), while IL-1Ra, Rho inhibitor I, and NSC23766 alone had no effect on OPC migration (Fig. 5E). These results further suggest a direct inhibitive effect of IL-1β on OPC migration through the IL-1R1 receptor.

3.3. The recruitment of OPCs contributes to oligodendrocyte regeneration and functional recovery

Although we observed increased recruitment of OPCs after the early treatment of IL-1Ra and *IL-1R1* knockout, we questioned whether the recruited OPCs could develop into mature oligodendrocytes and somehow benefit in functional recovery. First, BrdU
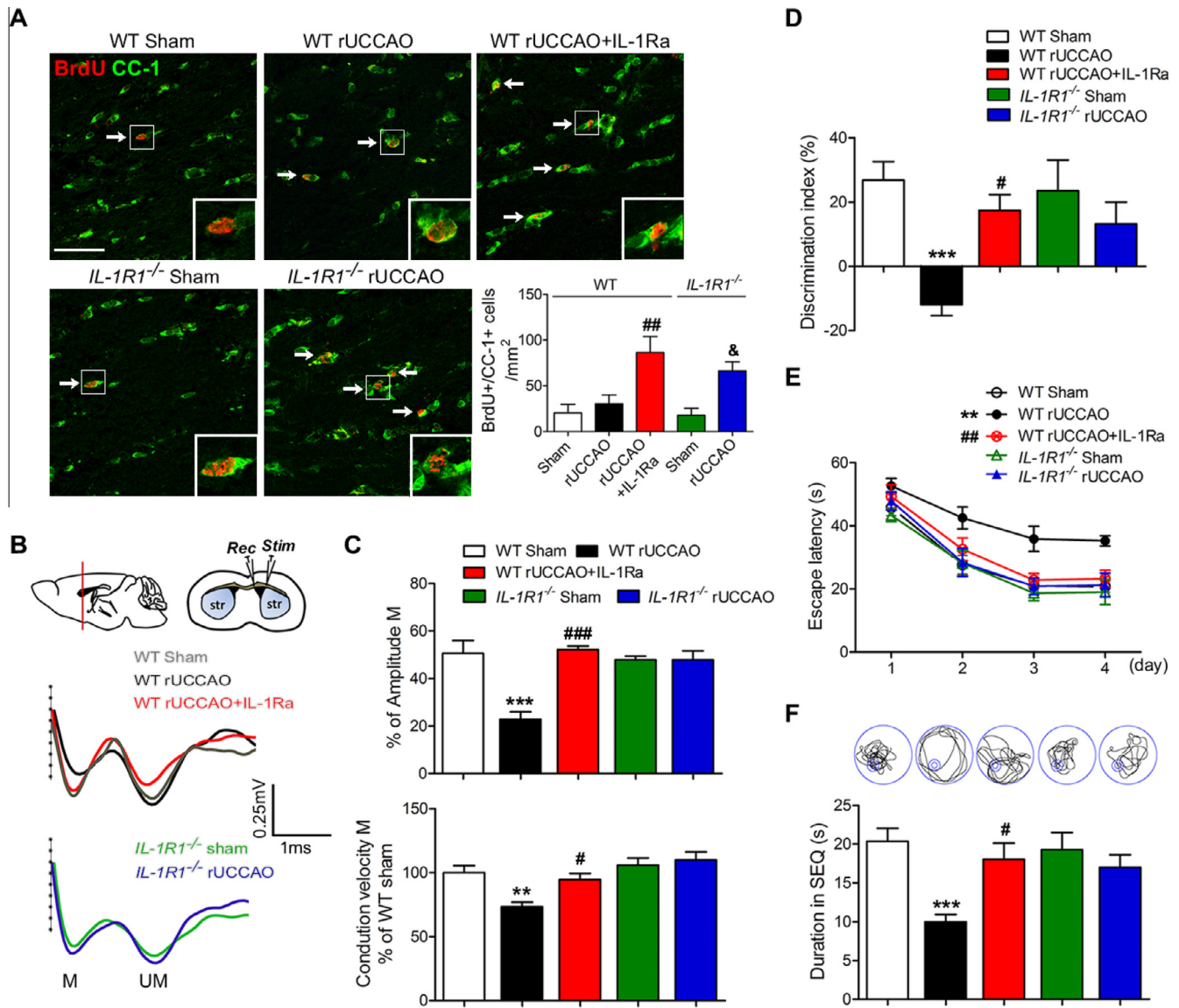
Fig. 6. The contribution of recruited OPCs to oligodendrocyte regeneration and functional recovery following chronic cerebral hypoperfusion. The number of newly generated mature oligodendrocytes (A) in the corpus callosum was counted at 34 d after rUCCAO (double BrdU+/CC-1+ cells are indicated by arrows, and the cells in the boxed portion are enlarged in the insets). A cartoon shows the position for recording electrode (Rec) and stimulating (Stim) electrode (B). Representative traces in B were obtained from CAP recording at 34 d after rUCCAO (M = myelinated fibers, UM = unmyelinated fibers). The maximal amplitudes of the first (A_M) and second waves (A_{UM}) were measured to estimate the amplitude percentage of myelinated fibers that were equal to $A_M/(A_M + A_{UM})$ (C). The conduction velocity of myelinated fibers was estimated (C). Cognitive behavior was evaluated from D28 to D34 after rUCCAO with the following tests: discrimination index in object recognition test (D), the latency to reach the platform during the acquisition trial in Morris water maze test (E), and searching time in the quadrant previously with platform (SEQ) in the probe trial (F) in Morris water maze test. Representative pictures of a searching track in the probe trial test are also shown in F. Scale bar, 50 μm. A, C: n = 4–5; D-F, n = 10–12. Data are represented as means ± SEM. [**]$P < 0.01$, [***]$P < 0.001$ vs. the sham group in WT mice; [#]$P < 0.05$, [##]$P < 0.01$, [###]$P < 0.001$ vs. the rUCCAO group in WT mice; [&]$P < 0.05$ vs. the sham group in $IL1R1^{-/-}$ mice.

+/CC-1+ double staining was performed at 34 d after rUCCAO to study the maturation of these recruited OPCs. We found that the early treatment of IL-1Ra and *IL-1R1* knockout both resulted in increased numbers of BrdU+/CC-1+ mature recruited OPCs (Fig. 6A). Secondly, we recorded the compound action potentials (CAP) produced by myelinated and unmyelinated fibers at 34 d after rUCCAO (Fig. 6B, C). In sham-operated WT brains, callosal stimulation produced a field response characterized by two distinct negative waves (the first corresponds to myelinated axons and the second corresponds to unmyelinated axons), both of which could be blocked by tetrodotoxin (TTX, preventing the firing of action potentials) and by the recision of callosum axons (Supplementary Fig. 5). A reduction of the CAP peak corresponding to myelinated axons was observed in the rUCCAO group of WT mice,

whereas the no change in the CAP peak was observed in either the IL-1Ra treatment group of WT mice or the *IL-1R1*−/− mice, and this was the case regardless of whether or not these mice received rUCCAO. Quantitative analysis of the percentage of CAP amplitude corresponding to myelinated axons (myelinated amplitude) and the conduction velocity of the first wave confirmed that blocking IL-1R1 promotes functional recovery in axonal signal propagation; this may result from an improvement in remyelination. Thirdly, mice were subjected to cognitive behavior tests, including object recognition tests and Morris water maze tests, which examine non-spatial working memory and spatial memory respectively, from D28 to D34 after rUCCAO (Fig. 6D–F), since the corpus callosum was associated with the cognitive behavior pertaining to both the non-spatial and spatial memory (Miu et al., 2006; Yoshizaki

et al., 2008). The rUCCAO group of WT mice showed a significant decrease in discriminative ability in the object recognition tests (Fig. 6D, $P < 0.001$), while mice that received IL-1Ra exhibited significant improvements in the discrimination index (Fig. 6D, $P < 0.05$). There were no differences between the sham and rUC-CAO groups of the $IL-1R1^{-/-}$ mice. In the Morris water maze tests, the rUCCAO group of WT mice demonstrated significantly longer escape latencies during the acquisition trials than did the sham-

operated group, but early treatment with IL-1Ra shortened escape latencies (Fig. 6E). In the probe trial for the water maze, when the platform was removed, the mice in the rUCCAO group spent less time searching in the quadrant previously with the platform compared with the sham group, revealing memory impairments. The IL-1Ra group had intact memory, evidenced by longer times spent in the quadrant that previously had a platform (Fig. 6F). However, $IL-1R1^{-/-}$ mice did not exhibit any differences in the acquisition
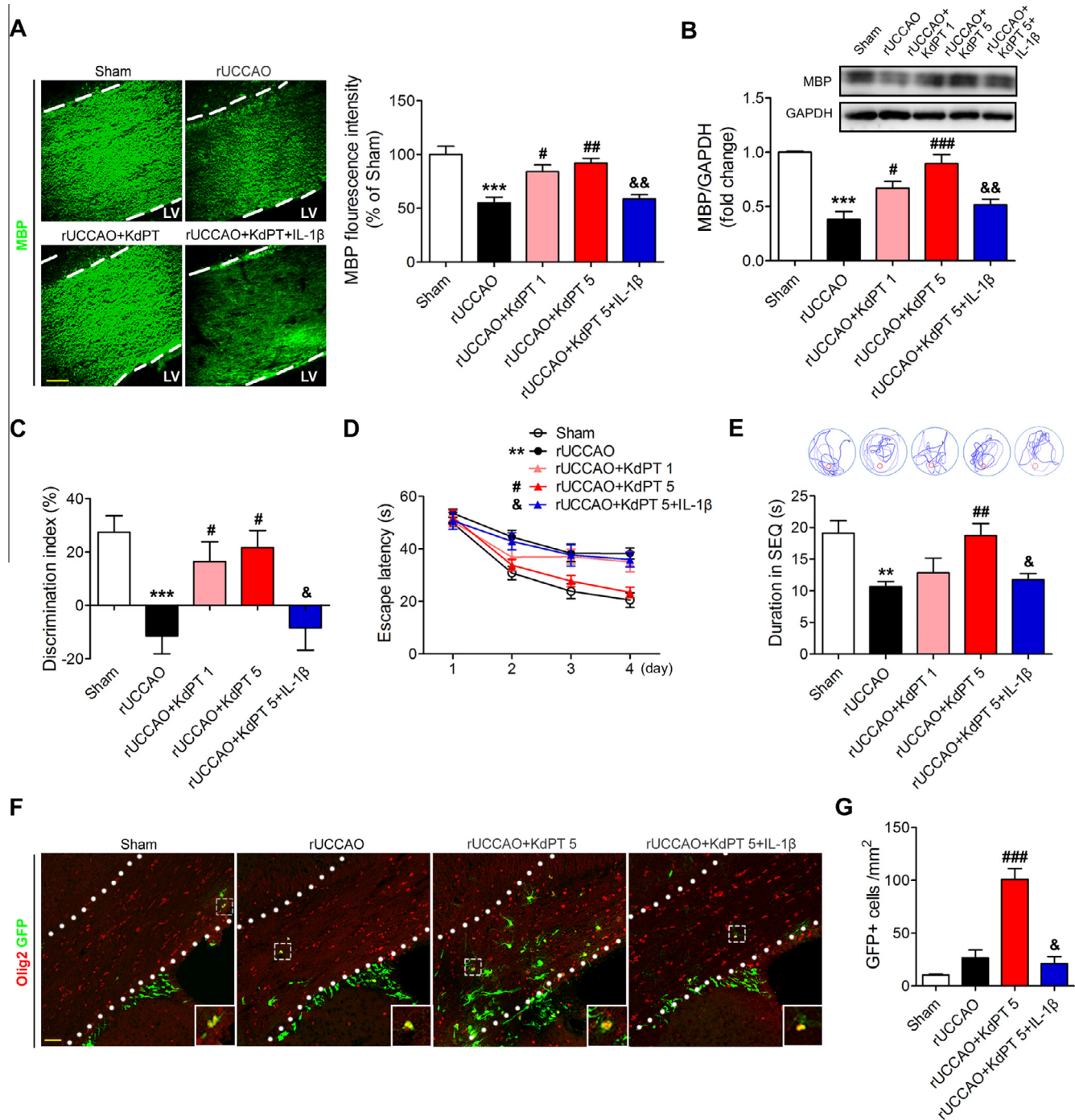
Fig. 7. KdPT alleviates white matter damage and promotes SVZ-derived OPC recruitment following chronic cerebral hypoperfusion. The MBP expression (on D34, A: immunostaining; B: western blot) and cognitive abilities (from D28 to D34, C: object recognition test; D: the acquisition trial in Morris water maze test; E: the probe trial in Morris water maze test) was determined after KdPT injections (1 or 5 mg/kg, i.p.) or co-treatment with IL-1β (3 ng in 1 μl saline, i.c.v) from D1 to D7. The number of SVZ-derived GFP+ cells in the corpus callosum at 8 d after rUCCAO was counted after KdPT injections (1 or 5 mg/kg, i.p.) or co-treatment with IL-1β (3 ng in 1 μl saline, i.c.v) from D1 to D7 (G), with representative photomicrographs in F. Scale bar, 50 μm. A, B: n = 4–5; C–E: n = 10–12; G: n = 4. Data are represented as means ± SEM. $^{**}P < 0.01$, vs. the sham group; $^{#}P < 0.05$, $^{##}P < 0.01$, $^{###}P < 0.001$ vs. the rUCCAO group; $^{&}P < 0.05$, $^{&&}P < 0.01$ vs. the rUCCAO + KdPT 5 group.

trials or probe trial, regardless of they whether or not they received rUCCAO (Fig. 6E–F). These results suggest that the increased recruitment of OPCs following inhibition of IL-1R1 benefits both oligodendrocyte regeneration and functional recovery.

3.4. KdPT promotes functional recovery and OPC recruitment to white matter following chronic cerebral hypoperfusion

Even though blocking IL-1R1 promotes remyelination and functional recovery following chronic cerebral hypoperfusion, the direct application of IL-1Ra in the clinic may be limited because it cannot cross the blood brain barrier (BBB). KdPT, the L-enantiomer of which is homologous to the amino acids 193–195 of IL-1β, can suppress IL-1R1 activation mediated NF-kB activation (Ferreira et al., 1988; Haddad et al., 2001; Mastrofrancesco et al., 2010). Intraperitoneal injection of KdPT alleviated brain damage after experimental traumatic brain injury in mice (Schaible et al., 2013). Here, monitoring of MBP expression revealed that administration of KdPT (1 or 5 mg/kg, i.p.) from 1 d to 7 d after surgery attenuated white matter damage in mice (Fig. 7A, B). In cognitive tests, mice that have received KdPT displayed elevated discrimination index scores in the object recognition test (Fig. 7C), and showed improved performance in the Morris water maze test (Fig. 7D, E). This protection can be completely abrogated by a co-treatment of IL-1β. In agreement with our aforementioned findings, more migrated newly generated OPC cells (Olig2+/GFP+ cells) in the corpus callosum were observed in mice that received KdPT, which was reversed when the mice was co-treated with IL-1β (Fig. 7F, G). These data suggest that KdPT promotes OPC recruitment and benefits white matter repair and functional recovery after chronic cerebral hypoperfusion through blocking IL-1R1.

4. Discussion

IL-1β and its receptor IL-1R1 play important roles in innate immunity, as well as in normal tissue homeostasis. However, their actions on white matter damage after chronic cerebral hypoperfusion are largely unknown. In this study, we demonstrated that IL-1β highly expressed at the early stage following chronic cerebral hypoperfusion and inhibiting IL-1R1 via IL-1Ra treatment or *IL-1R1* knockout markedly promotes white matter repair and alleviates cognitive impairments, which implies that IL-1β plays a detrimental role in the white matter repair. Therefore, IL-1R1 can be viewed as a therapeutic target for SIVD and its inhibitors may have potential uses in the treatment.

In the present study, we found that IL-1Ra treatment and *IL-1R1* knockout have no effect on the percentage of myelinated axons at the early stage following chronic cerebral hypoperfusion (Supplementary Fig. 3), but both increased the percentage of myelinated axons (i.e., remyelinated axons) at later stage (Fig. 2). Also, the apoptosis status of oligodendrocytes was unchanged after IL-1Ra treatment (Supplementary Fig. 4). These results suggest that IL-1β impedes remyelination following chronic cerebral hypoperfusion to inhibit white matter repair via IL-1R1. Remyelination can result from the proliferation and recruitment of newly generated OPCs to the demyelinating lesions and then the differentiation into myelins (Keirstead and Blakemore, 1999; Maki et al., 2013). Postmortem human brain studies have shown that, in ischemic white matter lesions of vascular dementia patients, the number of OPCs increases, but the number of mature oligodendrocytes decreases (Ekonomou et al., 2011; Miyamoto et al., 2010), suggesting that recruitment or differentiation is inhibited after chronic cerebral hypoperfusion. The SVZ and corpus callosum are the main sources of OPCs for remyelination (Franklin and Goldman, 2015). In the present study, a significant proliferation of OPCs was only

found in SVZ but not in corpus callosum at the early stage after chronic cerebral hypoperfusion (Fig. 3C–H). However, the newly generated OPCs in SVZ cannot recruit to corpus callosum (Fig. 4) and the spontaneous remyelination was blocked thereafter (Fig. 2C–E). Since the increased number of recruited OPCs that result from blocking IL-1R1 can be differentiated into mature OPCs after rUCCAO (Fig. 6A), it suggests that the recruitment of OPCs, but not the proliferation and differentiation of OPCs, is the only compromised step of remyelination following chronic cerebral ischemia. Promoting the recruitment of OPC to the lesions has been found to facilitate the regeneration of oligodendrocytes in a different demyelination mouse model (Boyd et al., 2013). Therefore, the discovery of inhibitory factors acting on OPC recruitment at early stage may enable endogenous regenerative progress to achieve functional recovery for the therapy of SIVD.

Our results showed that the inhibition of IL-1R1 by IL-1Ra treatment or *IL-1R1* knockout did not affect the proliferation of OPCs in SVZ (Fig. 3), but remarkably increased the number of newly generated OPCs (NG2+/BrdU+) in the corpus callosum (Fig. 4A, B). It implies that IL-1β impedes the recruitment of OPCs from SVZ to the corpus callosum via IL-1R1. This notion was further confirmed by retrovirus injection into SVZ, which is used to trace SVZ-derived OPCs. The results showed that IL-1Ra treatment and *IL-1R1* knockout increased the number of GFP+ SVZ-derived OPCs in the corpus callosum (Fig. 4C, D). The increase can be abrogated by IL-1β or by compensatory expression of IL-1R1 in *IL-1R1^{−/−}* mice (Fig. 4C–F). In transwell chamber assay, IL-1β inhibits the migration of OPCs via IL-1R1 (Fig. 5). Therefore, IL-1β/IL-1R1 is critical for the failure of white matter repair following chronic cerebral hypoperfusion; IL-1β acts through the downregulation of OPC recruitment to damaged white matter.

Although it has been reported that mice exposed to IL-1β had a long-lasting myelination defect through a blockage of the oligodendrocyte differentiation process in newborn mice (Favrais et al., 2011), here, we found no direct evidence for an effect of IL-1β/IL-1R1 on the differentiation of oligodendrocytes. However, if the differentiation is inhibited by IL-1β, the number of newly generated OPCs in the corpus callosum may be decreased or not changed after IL-1Ra delivery or in the *IL-1R1^{−/−}* mice due to the promotion of differentiation, which is opposite to our findings (Fig. 4A). So, it further indicates that recruitment but not differentiation is a crucial aspect of the failure of remyelination in the presence of IL-1β following chronic cerebral hypoperfusion. The discovery of factors that govern OPC recruitment is actually relatively rare as compared with the diverse array of extrinsic or intrinsic factors that have been suggested to regulate OPC proliferation and differentiation (Lopez Juarez et al., 2015). Accumulating evidence suggests that neuroinflammatory responses modulate pathological changes in white matter such as demyelination and remyelination (Barrette et al., 2013; Franklin and Goldman, 2015). The activation of astrocytes and microglia occur alongside a decrease in oligodendrocyte number in a kind of SIVD known as Binswanger's disease (Akiguchi et al., 1997). This has motivated research about how neuroinflammation contributes to SIVD. Here, we identified an inflammatory factor, IL-1β, from astrocytes and microglia that confers a detrimental effect on white matter repair following chronic cerebral hypoperfusion by inhibiting a critical step for remyelination: the inhibition of the chemotactic ability of OPC. Since CXCL1/CXCR2 has been reported to arrest OPC migration in developing spinal cord (Tsai et al., 2002) and CXCL1 expression can be induced in astrocytes by IL-1β (Omari et al., 2006), an indirect action of IL-1β on OPC recruitment cannot be completely excluded, that awaits further studies. The investigation of the role of cellular specific IL-1R1 by using conditional knockout mice would be undertaken in future to clarify this concern. Taken together, inhibition of its receptor IL-1R1 can promote OPC

recruitment and thereby improve remyelination that may be of benefit in therapies for SIVD.

IL-1Ra has been used in the treatment of rheumatoid arthritis, but its poor ability to penetrate the BBB motivated us to search for other approaches to block IL-1R1. The tripeptide KdPT exerts antagonistic activity against IL-1R1 (Getting et al., 2003; Haddad et al., 2001; Mastrofrancesco et al., 2010). Importantly, peripheral administration of KdPT, which can function in the brain (Schaible et al., 2013), provided comparable protection with IL-1Ra in terms of white matter damage and cognitive abilities, and also promoted the recruitment of SVZ-derived OPC cells (Figs. 2, 6 and 7). These actions can be completely abrogated, when the mice were co-treated with exogenous IL-1β. This implies that blocking IL-1R1, such as the application of KdPT, may have potential uses in the treatment of SIVD. Moreover, the upregulation of IL-1β only takes place during the early stages following chronic cerebral ischemia. Early treatment with either IL-1Ra or KdPT results in the alleviation of pathological and behavioral impairments, which suggests that early stage intervention is critical for the treatment of SIVD.

5. Conclusion

Our results suggest that the recruitment of OPCs, but not the proliferation and differentiation of OPCs, is the only compromised step of remyelination following chronic cerebral ischemia. IL-1β upregulated in the early stages impedes OPC recruitment via IL-1R1, which inhibits white matter repair and functional recovery. So, IL-1R1 can be seen as a therapeutic target for SIVD, and its inhibitors, such as KdPT, can be considered to be drugs with potential uses in the treatment of SIVD.

Acknowledgments

Appendix A. Supplementary data

Supplementary data associated with this article can be found, in the online version, at http://dx.doi.org/10.1016/j.bbi.2016.09.024.

References

Akiguchi, I., Tomimoto, H., Suenaga, T., Wakita, H., Budka, H., 1997. Alterations in glia and axons in the brains of Binswanger's disease patients. Stroke 28, 1423–1429.

Anliker, B., Choi, J.W., Lin, M.E., Gardell, S.E., Rivera, R.R., Kennedy, G., Chun, J., 2013. Lysophosphatidic acid (LPA) and its receptor, LPA1, influence embryonic Schwann cell migration, myelination, and cell-to-axon segregation. Glia 61, 2009–2022.

Arnett, H.A., Mason, J., Marino, M., Suzuki, K., Matsushima, G.K., Ting, J.P., 2001. TNF alpha promotes proliferation of oligodendrocyte progenitors and remyelination. Nat. Neurosci. 4, 1116–1122.

Barrette, B., Nave, K.A., Edgar, J.M., 2013. Molecular triggers of neuroinflammation in mouse models of demyelinating diseases. Biol. Chem. 394, 1571–1581.

Boyd, A., Zhang, H., Williams, A., 2013. Insufficient OPC migration into demyelinated lesions is a cause of poor remyelination in MS and mouse models. Acta Neuropathol. 125, 841–859.

Ekonomou, A., Ballard, C.G., Pathmanaban, O.N., Perry, R.H., Perry, E.K., Kalaria, R.N., Minger, S.L., 2011. Increased neural progenitors in vascular dementia. Neurobiol. Aging 32, 2152–2161.

El Waly, B., Macchi, M., Cayre, M., Durbec, P., 2014. Oligodendrogenesis in the normal and pathological central nervous system. Front. Neurosci. 8, 145.

Favrais, G., van de Looij, Y., Fleiss, B., Ramanantsoa, N., Bonnin, P., Stoltenburg-Didinger, G., Lacaud, A., Saliba, E., Dammann, O., Gallego, J., Sizonenko, S., Hagberg, H., Lelievre, V., Gressens, P., 2011. Systemic inflammation disrupts the developmental program of white matter. Ann. Neurol. 70, 550–565.

Ferreira, S.H., Lorenzetti, B.B., Bristow, A.F., Poole, S., 1988. Interleukin-1 beta as a potent hyperalgesic agent antagonized by a tripeptide analogue. Nature 334, 698–700.

Franklin, R.J., Goldman, S.A., 2015. Glia disease and repair-remyelination. Cold Spring Harb. Perspect. Biol. 7, a020594.

Getting, S.J., Schioth, H.B., Perretti, M., 2003. Dissection of the anti-inflammatory effect of the core and C-terminal (KPV) alpha-melanocyte-stimulating hormone peptides. J. Pharmacol. Exp. Ther. 306, 631–637.

Gootjes, L., Teipel, S.J., Zebuhr, Y., Schwarz, R., Leinsinger, G., Scheltens, P., Moller, H. J., Hampel, H., 2004. Regional distribution of white matter hyperintensities in vascular dementia, Alzheimer's disease and healthy aging. Dement. Geriatr. Cogn. Disord. 18, 180–188.

Haddad, J.J., Lauterbach, R., Saade, N.E., Safieh-Garabedian, B., Land, S.C., 2001. Alpha-melanocyte-related tripeptide, Lys-D-Pro-Val, ameliorates endotoxin-induced nuclear factor kappaB translocation and activation: evidence for involvement of an interleukin-1beta193-195 receptor antagonism in the alveolar epithelium. Biochem. J. 355, 29–38.

Hayakawa, K., Pham, L.D., Som, A.T., Lee, B.J., Guo, S., Lo, E.H., Arai, K., 2011. Vascular endothelial growth factor regulates the migration of oligodendrocyte precursor cells. J. Neurosci. 31, 10666–10670.

Huang, J., Upadhyay, U.M., Tamargo, R.J., 2006. Inflammation in stroke and focal cerebral ischemia. Surg. Neurol. 66, 232–245.

Kako, E., Kaneko, N., Aoyama, M., Hida, H., Takebayashi, H., Ikenaka, K., Asai, K., Togari, H., Sobue, K., Sawamoto, K., 2012. Subventricular zone-derived oligodendrogenesis in injured neonatal white matter in mice enhanced by a nonerythropoietic erythropoietin derivative. Stem cells 30, 2234–2247.

Kalaria, R.N., Maestre, G.E., Arizaga, R., Friedland, R.P., Galasko, D., Hall, K., Luchsinger, J.A., Ogunniyi, A., Perry, E.K., Potocnik, F., Prince, M., Stewart, R., Wimo, A., Zhang, Z.X., Antuono, P.World Federation of Neurology Dementia Research, G., 2008. Alzheimer's disease and vascular dementia in developing countries: prevalence, management, and risk factors. Lancet Neurol. 7, 812–826.

Keirstead, H.S., Blakemore, W.F., 1999. The role of oligodendrocytes and oligodendrocyte progenitors in CNS remyelination. Adv. Exp. Med. Biol. 468, 183–197.

Le Clainche, C., Carlier, M.F., 2008. Regulation of actin assembly associated with protrusion and adhesion in cell migration. Physiol. Rev. 88, 489–513.

Liebetanz, D., Merkler, D., 2006. Effects of commissural de- and remyelination on motor skill behaviour in the cuprizone mouse model of multiple sclerosis. Exp. Neurol. 202, 217–224.

Lopez Juarez, A., He, D., Richard Lu, Q., 2015. Oligodendrocyte progenitor programming and reprogramming: toward myelin regeneration. Brain Res. 1638, 209–220.

Ma, J., Xiong, J.Y., Hou, W.W., Yan, H.J., Sun, Y., Huang, S.W., Jin, L., Wang, Y., Hu, W. W., Chen, Z., 2012. Protective effect of carnosine on subcortical ischemic vascular dementia in mice. CNS Neurosci. Ther. 18, 745–753.

Ma, J., Zhang, J., Hou, W.W., Wu, X.H., Liao, R.J., Chen, Y., Wang, Z., Zhang, X.N., Zhang, L.S., Zhou, Y.D., Chen, Z., Hu, W.W., 2015. Early treatment of minocycline alleviates white matter and cognitive impairments after chronic cerebral hypoperfusion. Sci. Rep. 5, 12079.

Maki, T., Liang, A.C., Miyamoto, N., Lo, E.H., Arai, K., 2013. Mechanisms of oligodendrocyte regeneration from ventricular-subventricular zone-derived progenitor cells in white matter diseases. Front. Cell. Neurosci. 7, 275.

Mason, J.L., Suzuki, K., Chaplin, D.D., Matsushima, G.K., 2001. Interleukin-1beta promotes repair of the CNS. J. Neurosci. 21, 7046–7052.

Mastrofrancesco, A., Kokot, A., Eberle, A., Gibbons, N.C., Schallreuter, K.U., Strozyk, E., Picardo, M., Zouboulis, C.C., Luger, T.A., Bohm, M., 2010. KdPT, a tripeptide derivative of alpha-melanocyte-stimulating hormone, suppresses IL-1 beta-mediated cytokine expression and signaling in human sebocytes. J. Immunol. 185, 1903–1911.

Miu, A.C., Heilman, R.M., Pasca, S.P., Stefan, C.A., Spanu, F., Vasiu, R., Olteanu, A.I., Miclea, M., 2006. Behavioral effects of corpus callosum transection and environmental enrichment in adult rats. Behav. Brain Res. 172, 135–144.

Miyamoto, N., Tanaka, R., Shimura, H., Watanabe, T., Mori, H., Onodera, M., Mochizuki, H., Hattori, N., Urabe, T., 2010. Phosphodiesterase III inhibition promotes differentiation and survival of oligodendrocyte progenitors and enhances regeneration of ischemic white matter lesions in the adult mammalian brain. J. Cereb. Blood Flow Metab. 30, 299–310.

Omari, K.M., John, G., Lango, R., Raine, C.S., 2006. Role for CXCR2 and CXCL1 on glia in multiple sclerosis. Glia 53, 24–31.

Ozerdem, U., Grako, K.A., Dahlin-Huppe, K., Monosov, E., Stallcup, W.B., 2001. NG2 proteoglycan is expressed exclusively by mural cells during vascular morphogenesis. Dev. Dynam. 222, 218–227.

Schaible, E.V., Steinstrasser, A., Jahn-Eimermacher, A., Luh, C., Sebastiani, A., Kornes, F., Pieter, D., Schafer, M.K., Engelhard, K., Thal, S.C., 2013. Single administration of tripeptide alpha-MSH(11-13) attenuates brain damage by reduced inflammation and apoptosis after experimental traumatic brain injury in mice. PLoS One 8, e71056.

Selnes, O.A., Vinters, H.V., 2006. Vascular cognitive impairment. Nat. Clin. Pract. Neurol. 2, 538–547.

Singh, R., Wang, B., Shirvaikar, A., Khan, S., Kamat, S., Schelling, J.R., Konieczkowski, M., Sedor, J.R., 1999. The IL-1 receptor and Rho directly associate to drive cell activation in inflammation. J. Clin. Invest. 103, 1561–1570.

Tsai, H.H., Frost, E., To, V., Robinson, S., Ffrench-Constant, C., Geertman, R., Ransohoff, R.M., Miller, R.H., 2002. The chemokine receptor CXCR2 controls

positioning of oligodendrocyte precursors in developing spinal cord by arresting their migration. Cell 110, 373–383.

Vela, J.M., Molina-Holgado, E., Arevalo-Martin, A., Almazan, G., Guaza, C., 2002. Interleukin-1 regulates proliferation and differentiation of oligodendrocyte progenitor cells. Mol. Cell. Neurosci. 20, 489–502.

Wakita, H., Tomimoto, H., Akiguchi, I., Matsuo, A., Lin, J.X., Ihara, M., McGeer, P.L., 2002. Axonal damage and demyelination in the white matter after chronic cerebral hypoperfusion in the rat. Brain Res. 924, 63–70.

Yoshizaki, K., Adachi, K., Kataoka, S., Watanabe, A., Tabira, T., Takahashi, K., Wakita, H., 2008. Chronic cerebral hypoperfusion induced by right unilateral common carotid artery occlusion causes delayed white matter lesions and cognitive impairment in adult mice. Exp. Neurol. 210, 585–591.

Zuliani, G., Ranzini, M., Guerra, G., Rossi, L., Munari, M.R., Zurlo, A., Volpato, S., Atti, A.R., Ble, A., Fellin, R., 2007. Plasma cytokines profile in older subjects with late onset Alzheimer's disease or vascular dementia. J. Psychiatr. Res. 41, 686–693.